SUPPORTING INFORMATION

An *Operando* Investigation of (Ni-Fe-Co-Ce)O$_x$ System as Highly Efficient Electrocatalyst for Oxygen Evolution Reaction

Marco Favaro[‡1,2,3], Walter S. Drisdell[‡2,3], Matthew A. Marcus[1], John M. Gregoire,[4] Ethan J. Crumlin[1,*], Joel A. Haber[4,*], Junko Yano[2,3,5,*]

[1] *Advanced Light Source, Lawrence Berkeley National Laboratory, One Cyclotron Rd., Berkeley, CA 94720, USA.*
[2] *Joint Center for Artificial Photosynthesis, Lawrence Berkeley National Laboratory, One Cyclotron Rd., Berkeley, CA 94720, USA.*
[3] *Chemical Sciences Division, Lawrence Berkeley National Laboratory, One Cyclotron Rd., Berkeley, CA 94720, USA.*
[4] *Joint Center for Artificial Photosynthesis, California Institute of Technology; Pasadena, CA 91125, USA.*
[5] *Molecular Biophysics and Integrated Bioimaging Division, Lawrence Berkeley National Laboratory, One Cyclotron Rd., Berkeley, CA 94720.*

*Correspondence to: Ethan J. Crumlin (ejcrumlin@lbl.gov), Joel A. Haber (jahaber@caltech.edu) and Junko Yano (jyano@lbl.gov).

[‡] These two authors equally contributed to the work.

S1. Experimental

S1.1. Sample preparation

S1.1.1. Preparation of Precursor Ink Solutions

Four separate metal inks were prepared by mixing 5 mmoles of each of the metal precursors (Ni(NO$_3$)$_2$–6H$_2$O (99.999%), Fe(NO$_3$)$_3$–9H$_2$O (≥98%), Co(NO$_3$)$_2$–6H$_2$O (99.99%,), and Ce(NO$_3$)$_3$–6H$_2$O (99.99%)) with 0.80 g Pluronic F127 (Aldrich), 1.0 mL glacial acetic acid, 0.40 mL of concentrated HNO$_3$, and 30 mL of 200 proof ethanol.

S1.1.2. Preparation of Catalyst on Fluorine-doped Tin Oxide

The seperate Ni, Fe, Co, and Ce inks were loaded into separate channels and printed at 2880 x 1440 dpi with the volume ratios required to yield Ni$_{0.3}$Fe$_{0.07}$Co$_{0.2}$Ce$_{0.43}$O$_x$. The inks were allowed to mix on the substrate before drying. The metals were deposited at a loading of 7.5 nmol/mm^2. The ink was dried and the metal precursors converted to metal oxides by calcination in air at 37 °C for 20 h, then at 67 °C for 26 h, followed by a 5 h ramp and 10 h soak at 350 °C. The catalyst compositions characterized in Figure 1 are provided in Table S1, and were similarly prepared as 1 mm2 sample spots at a loading of 3.8 nmol/mm^2, as described in reference 39.[1]

S1.1.3. Preparation of Catalyst on Glassy Carbon

The selected composition (Ni$_{0.3}$Fe$_{0.07}$Co$_{0.2}$Ce$_{0.43}$O$_x$) was printed onto thin glassy carbon window electrodes (10 mm x 10 mm x 0.5 mm, SIGRADUR G, HTW Hochtemperatur-Werkstoffe GmbH), which were cleaned with 18 MΩ-cm water, and then ethanol and dried with a stream of compressed air before use. A single, mixed metal composition ink was prepared by mixing the

single metal inks described in 2.1.1.: 9.0 mL of the Ni ink + 2.1 mL Fe ink + 6 mL Co ink + 12.9 mL Ce ink. The mixed-metal ink was a stable, clear solution after mixing without signs of precipitation. The ink was loaded into one channel of the modified ink jet printer and printed onto the glassy carbon windows at 2880 x 1440 dpi, for a total metal loading of 3.8 nmol/mm^2. The ink was dried and the metal precursors converted to metal oxides by calcination in air at 37 °C for 20 h, then at 67 °C for 26 h, followed by a 5 h ramp and 10 h soak at 350 °C.

Table S1. Catalyst compositions along the 3 composition lines shown in Figure 1a. A CV for each of these compositions is shown in Figure 1b-1d.

end-point of composition line	Ni	Fe	Co	Ce
Ni-Fe	0.50	0.50	0.00	0.00
	0.50	0.43	0.07	0.00
	0.50	0.30	0.20	0.00
	0.53	0.20	0.27	0.00
	0.57	0.10	0.33	0.00
Ni-Co	0.57	0.00	0.43	0.00
Ni-Co	0.57	0.00	0.43	0.00
	0.53	0.00	0.37	0.10
	0.47	0.00	0.37	0.17
	0.43	0.00	0.33	0.23
	0.37	0.00	0.33	0.30
	0.33	0.00	0.27	0.40
Ni-Co-Ce	0.27	0.00	0.23	0.50
Ni-Fe	0.50	0.50	0.00	0.00
	0.43	0.37	0.10	0.10
	0.43	0.23	0.17	0.17
	0.40	0.17	0.20	0.23
	0.33	0.17	0.20	0.30
	0.30	0.13	0.20	0.37
	0.30	0.07	0.20	0.43
Ni-Co-Ce	0.27	0.00	0.23	0.50

S1.2. Beamline 9.3.1 (ALS) and *operando* APXPS experimental details

The beamline is equipped with a bending magnet and a Si (111) double crystal monochromator (DCM), with a total energy range between 2 and 7 keV ("tender" X-ray range).[2] The analyzer (R4000 HiPP-2, Scienta) pass energy was set to 200 eV, using a step of 100 meV and a dwell time of 200 µs. The measurements were taken using a photon energy of 4.0 keV at room temperature (r.t.) and in normal emission (NE), at a pressure (of water vapor) ranging from 16 to 18 torr. Under these conditions, the spectral resolution at 4.0 keV is equal to 250 meV. The calibration of the binding energy (BE) scale was carried out using the Au 4f photoemission peak as reference (4f$_{7/2}$ BE = 84.0 eV). All the fits reported in this work have been carried out using a Doniach-Šunjić shape for the Au 4f and Ce 3d photoemission peaks, and a symmetrical Voigt function for the Ni 2p, Co 2p, Fe 2p and O 1s photoemission peaks (after Shirley background subtraction). The former

have been fitted accordingly to the well-established multiplet splitting procedure.[3] The χ^2 minimization was ensured by the use of a nonlinear least squares routine.

S1.2.1. Electrochemical measurements and Dip and Pull method

The chemicals employed here were high purity reagents and were used as-received without further purification. The electrolytes were prepared using MilliQ water (DI, ρ=18.2 MΩ·cm), KOH (99.99%, Aldrich), and KF (Aldrich, 99.99%). The counter electrode (CE, Pt polycrystalline foil, Aldrich) was polished to a mirror finish using silicon carbide papers with decreasing grain size (Struers, grit: 2400 and 4000). The CE was then cleaned by sonicating it in a 1:1 mixture of MilliQ water/ethanol (Aldrich, 1:1) for 10 min, two times, then in pure MilliQ water for 15 min, thoroughly rinsing with MilliQ water, and blowing dry with a N_2 stream. The working electrodes (WEs) were constituted by the OER electrocatalyst with a nominal formula $Ni_{0.3}Fe_{0.07}Co_{0.2}Ce_{0.43}O_x$, prepared via ink-jet deposition on 250 nm thick fluorine-doped tin oxide (FTO) on a glass substrate (Aldrich, see **section 1.1.2**). Before every experiment, the received electrodes were thoroughly rinsed with MilliQ water, dried for 15 min in a N_2 stream, and finally placed in high vacuum (about 10^{-3} mtorr) for 1 hour. A leakless miniaturized Ag/AgCl/Cl$^-_{(sat)}$ (EDAQ, ET072-1) was used as the reference electrode (RE). All the potentials reported in this study are relative to this RE ($E^{\varnothing}_{Ag/AgCl}$ = +197 mV vs. SHE). Prior to its introduction into the main chamber, the electrolyte (1.0 M KOH + 0.1 M KF) was outgassed for at least 30 min at low pressure (around 12 torr) in a dedicated off-line chamber. Then, once the manipulator and the outgassed electrolyte were placed into the main chamber of the APXPS endstation, the pressure was carefully reduced to the water vapor tension value (between 16 and 20 torr, at r.t.); finally, the dip and pull procedure was carried out in order to obtain a stable and conductive nanometer-thick electrolyte layer on the WE surface (**Figure 2**).[2,4,5] The electrochemical data were recorded using a Biologic SP 300 potentiostat/galvanostat.

S1.3. Beamline 10.3.2 (ALS), 7-3 (SSRL) and *operando* XAS experimental details

S1.3.1. *Operando* XANES

Operando X-ray Absorption Near Edge Structure (XANES) measurements were performed at beamline 10.3.2 at the Advanced Light Source (ALS) at Lawerence Berkeley National Laboratory. This beamline uses a bending magnet source and a Si(111) double crystal monochromator to provide tunable X-rays between 2.1 – 17 keV with a flux of ~ 9 x 10^9 photons/s and a resolving power (E/ΔE) of 7000 at 10.0 keV. The X-ray spot size was 10 μm by 2 μm at the sample. This small spot size, coupled with a precision motorized sample stage, allows μm-scale chemical mapping. A 7-element solid-state Ge fluorescence detector (UltraLEGe, Canberra) was used to collect XANES spectra and chemical maps in fluorescence yield mode.

For these measurements, glassy carbon plates (10 x 10 x 0.5 mm, Sigradur G, HTW) were used instead of silicon nitride windows, serving as substrates for the samples. These plates were attached to the cells using fast-curing epoxy (Devcon), and electrical contact was made to the back side using Cu tape. Otherwise, cell operation was the same as reported previously; briefly, X-ray photons entered the cell through the back side of the glassy carbon plate, and fluoresced photons were detected exiting through the glassy carbon plate at 90 degrees relative to the incident beam. This allows collection of XANES spectra of the catalyst while running electrochemistry in the cell.

1.0M KOH solution was used for the electrolyte and a Biologic SP 300 potentiostat/galvanostat was used for electrochemical control.

S1.3.2. *Operando* EXAFS

Operando Extended X-ray Absorption Fine Structure (EXAFS) measurements were performed at beamline 7-3 at the Stanford Synchrotron Radiation Lightsource (SSRL) at SLAC National Accelerator Laboratory. This beamline features a wiggler source and a Si (220) double crystal monochromator to deliver X-rays between 4.6 – 37 keV in energy, with a resolving power (E/ΔE) of 1000. The photon flux is ~10^{12} photons/s with an unfocused beam 2 x 15 mm in size, reduced to 1 x 1 mm at the sample using slits. Fluorescence signal was collected using a 30-element Ge detector (Canberra).

EXAFS was collected using the same operando electrochemical cells and samples described in section 2.3.1, using the same operating procedures. Electrochemical control was maintained using a Biologic VSP potentiostat/galvanostat.

S1.3.3. *Ex situ* soft XAS

Ex situ soft X-ray absorption spectra were collected at beamline 6.3.1 at the ALS. This beamline features a bend magnet source and a variable line spacing plane grating monochromator (VLS-PGM) to provide X-rays between 250 – 2000 eV with a resolving power (E/ΔE) of 5000. The X-ray spot size at the sample is ~ 50 x 500 μm with a flux of ~10^{11} photons/s. Spectra were collected under ultra-high vacuum (UHV) conditions in total electron yield (TEY) mode by measuring replacement current through a picoammeter (Keithley).

Ex situ samples were prepared on glassy carbon discs (Sigradur G, HTW) as described in **section 1.1.3**. Spectra were collected for a pristine sample and a sample that had been subjected to electrochemistry.
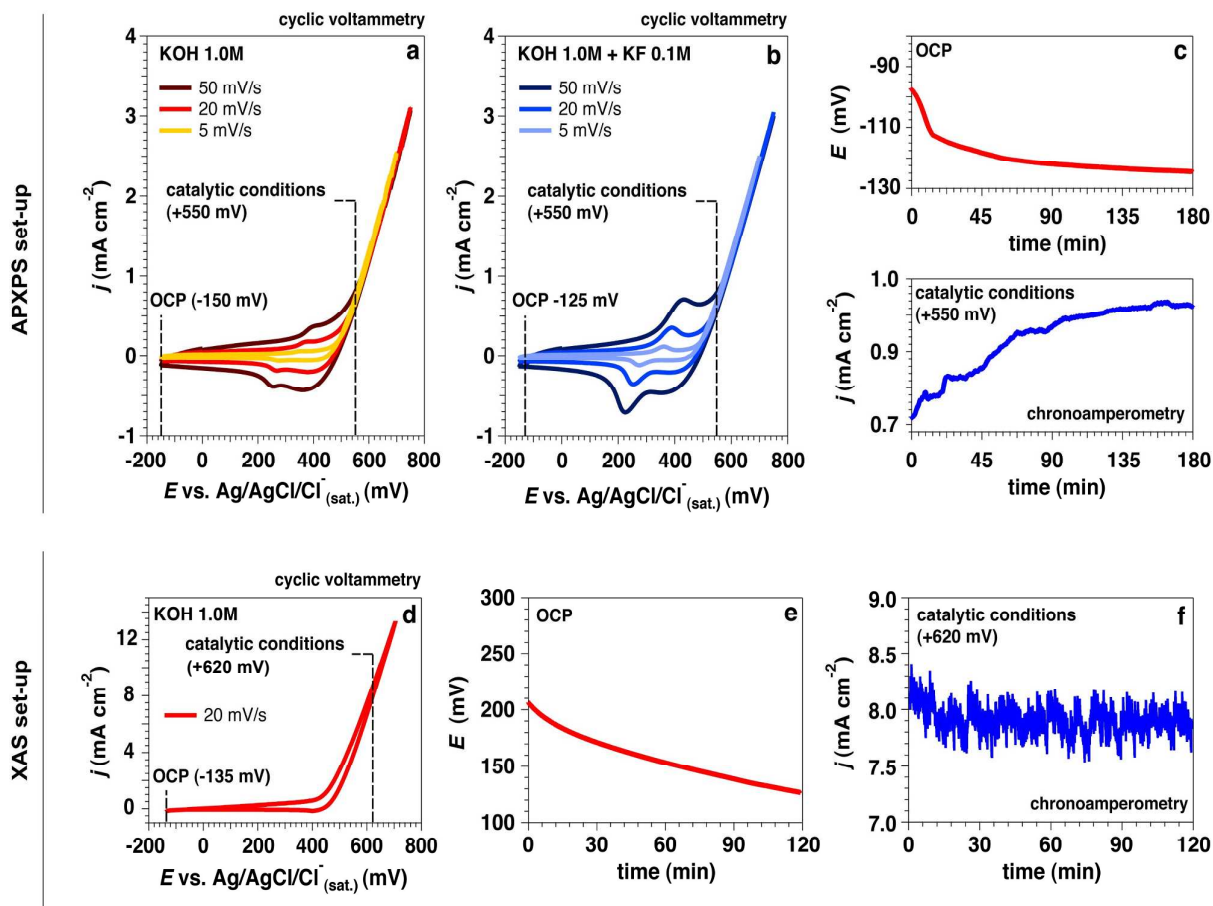
S2. Electrochemical characterization

Figure S1. a, b: cyclic voltammetries (CVs) acquired in the anodic region of the quinary metal oxide catalyst in KOH 1.0M and KOH 1.0M + KF 0.1M aqueous solutions, respectively, during the *operando* APXPS; **c**: time trends of the open circuit potential (OCP) and current density under catalytic conditions at +550 mV in KOH 1.0M, during the *operando* APXPS. The increasing surface hydrophilicity under catalytic conditions (due to undergoing oxidation processes) could lead to an upward movement of the liquid meniscus in our apparatus (see schematization reported in **Figure 2** for *operando* APXPS). Since the acquired currents are normalized by the geometric area (area of sample exposed to the electrolyte) under the assumption that the surface roughness is constant, the apparent increase of the catalytic activity (current density at constant potential over time) may be due to an increase of the surface roughness exposing more surface area to the electrolyte; **d, e, f**: CV and time trends of OCP and current density under catalytic conditions at +620 mV in KOH 1.0M during the *operando* XAS measurements, respectively.

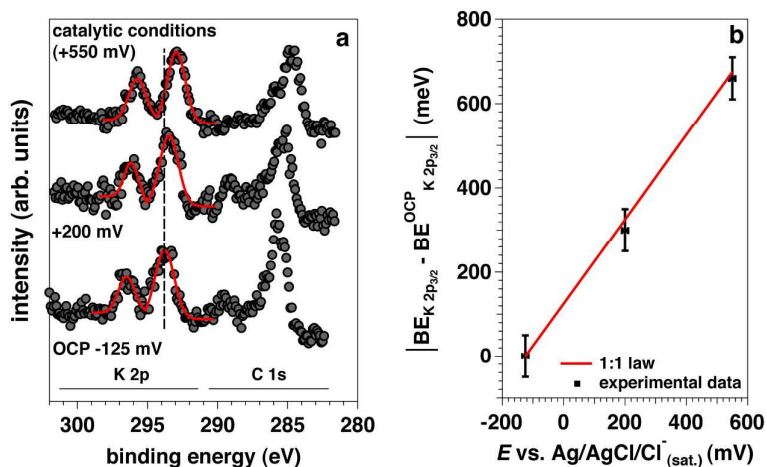# S3. Conductivity of the nanometric-thick electrolyte layer

Figure S2. a: K 2p photoemission peaks for different applied potentials at the WE, acquired in the KOH 1.0M + KF 0.1M electrolyte; **b**: comparison between the observed K $2p_{3/2}$ BE shift and the theoretical one (1:1 law), as a function of the applied potential (the BE shifts are referred to the initial value recorded at the OCP).

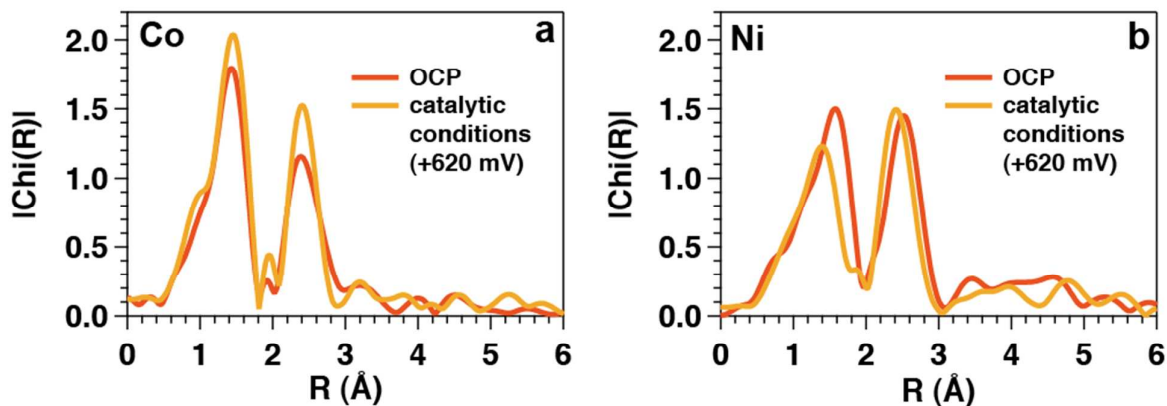# S4. *Operando* EXAFS at the Ni and Co K edges

Figure S3. a, b: Fourier-transformed EXAFS spectra at the Co and Ni K edges, respectively, at OCP and under catalytic conditions.
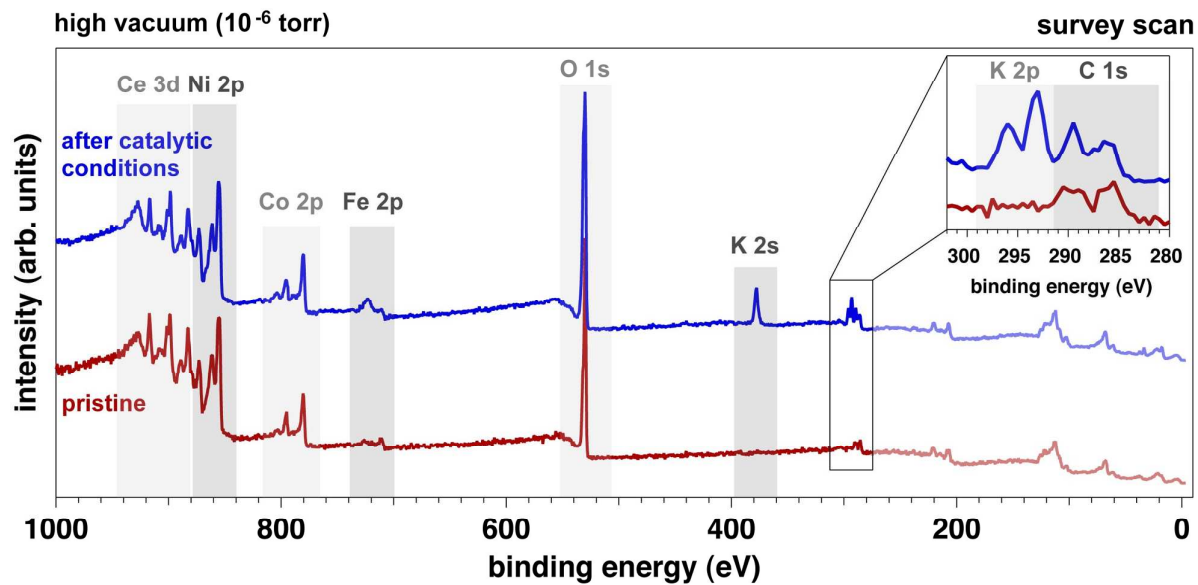
S5. *In situ* APXPS survey scans

Figure S4. XPS *in situ* survey scan acquired at a pressure of 10^{-6} torr and at a photon energy of 4000 eV, for the pristine material and after catalytic conditions (+550 mV).

S6. Comparison with literature

Table S2. Comparison between the data obtained in this study and previous work reported in literature using *in situ* or *operando* electron spectroscopies (APXPS and XAS).

	Ni	Fe	Co	Ce
XPS				
This study (*operando* APXPS, quasi *in situ* APXPS)	NiOx(OH)y	FeO(OH)	CoOx(OH)y	CeO$_2$
Weidler et al.,[74] **(films, *ex situ*)**	-	-	Sub-stoichiometric CoO(OH)	-
Klaus et al.,[92] **(films, *ex situ*)**	Sub-stoichiometric (Ni-Fe)O(OH)x	Sub-stoichiometric (Fe-Ni)O(OH)x	-	-
Ali-Löytty et al.,[94] **(films, *operando* APXPS)**	Sub-stoichiometric (Ni-Fe)O(OH)x	Sub-stoichiometric (Fe-Ni)O(OH)x	-	-
XAS				
This study (*in situ* XAS – *ex situ* XANES)	NiO(OH)	-	CoO(OH)	CeO$_2$
Bergmann et al.,[85] **(NPs, *in situ* XAS)**	-	-	Highly disordered, sub-stoichiometric CoOx(OH)y	-
Friebel et al.,[54] **(films, *in situ* XAS + DFT)**	(Ni-Fe)O(OH)	(Fe-Ni)O(OH)	-	-
Wang et al.,[60] **(NPs, in-situ XAS, *ex situ* XANES)**	Sub-stoichiometric (Ni-Fe)(OH)x	Sub-stoichiometric (Fe-Ni)(OH)x	-	-
Risch et al.,[84] **(films, *in situ* XAS and XRD)**	-	-	CoO(OH) + traces of Co (IV)	-
Friebel et al.,[53] **(films, *in situ* XAS)**	-	-	CoO(OH)	-
Indra et al.,[11] **(NPs, *in situ* XAS and XRD)**	-	-	Highly disordered sub-stoichiometric CoOx(OH)y	-
Kanan et al. [56] **(films, *in situ* XAS)**			CoO(OH) + possible Co (IV)	

References

(1)   Haber, J. A.; Xiang, C.; Guevarra, D.; Jung, S.; Jin, J.; Gregoire, J. M. *ChemElectroChem* 2014, *1*, 524-528.

(2)   Lichterman, M. F.; Richter, M. H.; Hu, S.; Crumlin, E. J.; Axnanda, S.; Favaro, M.; Drisdell, W.; Hussain, Z.; Brunschwig, B. S.; Lewis, N. S.; Liu, Z.; Lewerenz, H. J. *Journal of the Electrochemical Society* 2016, *163*, H139-H146.

(3)   Nyholm, R.; Martensson, N.; Lebugle, A.; Axelsson, U. *Journal of Physics F-Metal Physics* 1981, *11*, 1727-1733.

(4)   Wang, D.; Zhou, J.; Hu, Y.; Yang, J.; Han, N.; Li, Y.; Sham, T.-K. *The Journal of Physical Chemistry C* 2015, *119*, 19573-19583.

(5)   Lichterman, M. F.; Hu, S.; Richter, M. H.; Crumlin, E. J.; Axnanda, S.; Favaro, M.; Drisdell, W.; Hussain, Z.; Mayer, T.; Brunschwig, B. S.; Lewis, N. S.; Liu, Z.; Lewerenz, H. J. *Energy Environ. Sci.* 2015, *8*, 2409-2416.